Biosensors and Bioelectronics 24 (2009) 3043–3048

Contents lists available at ScienceDirect

Biosensors and Bioelectronics

journal homepage: www.elsevier.com/locate/bios

# Enhanced SPR response from patterned immobilization of surface bioreceptors on nano-gratings

X.D. Hoa[a,d], A.G. Kirk[b,e], M. Tabrizian[a,c,d,e,*]

[a] Department of Biomedical Engineering, McGill University, Montréal, Canada H3A 2B4
[b] Department of Electrical and Computer Engineering, McGill University, Montréal, Canada H3A 2A7
[c] Faculty of Dentistry, McGill University, Montreal, Canada H3A 2B2
[d] Centre for Biorecognition and Biosensors, McGill University, Montreal, Canada H3A 2B4
[e] McGill Institute for Advanced Materials, McGill University, Montreal, Canada H3A 2A7

ARTICLE INFO

*Article history:*
Received 18 December 2008
Received in revised form 10 March 2009
Accepted 11 March 2009
Available online 24 March 2009

*Keywords:*
Surface plasmon resonance biosensors
Nano-gratings
Self-assembled monolayer
Electron-beam lithography
Metal lift-off
Rigorous coupled-wave analysis

ABSTRACT

In this report, nano-gratings with guided adsorption of biomolecules are investigated as new transducer elements or biointerfaces for surface plasmon resonance biosensor technologies. SPR biosensors are of particular interest due to the interaction between the electromagnetic fields and periodic nano-structures. In this article, sensitivity enhancement is demonstrated for a surface plasmon resonance interface, in a Kretschmann's configuration, featuring nano-gratings combined with nano-patterned immobilization of surface bioreceptors. The fabrication of this enhanced biointerface is demonstrated using a combination of metal lift-off and self-assembled monolayers. Rigorous coupled-wave analyses point to an increase in SPR angular response for the immobilization of surface bioreceptors onto areas of the nano-corrugated surface exhibiting high electromagnetic field intensity. Experimental measurements of the immobilization of anti-TNF-α antibody as a model bioreceptor using an imaging-SPR technique show a 3 times increase in angular resonance response from nano-grating surfaces with functionalized mesas compared to a planar surface or to a uniformly functionalized nano-grating surface. Furthermore, results also show an increased detection of TNF-α due to the increased accessibility to the adsorbed bioreceptors on the nano-gratings.


## 1. Introduction

Today, the development of surface plasmon resonance (SPR) immunosensors or biosensors is increasingly focused on the integration of the system components for in-field biomedical, food and environmental applications. The interest in the SPR technology lies in its label-free and real-time biomolecular analysis. In many cases, the detection of low-molecular weight biomolecules (proteins, DNA) at low concentrations is sought, raising significant challenges for the design of various integrated biosensor components including the optical system, data-analysis method, and in particular the functionalized biointerface. For the latter, the literature presents several examples of surface engineering techniques developed to increase the surface binding affinity, capacity and specificity of SPR biosensors and other immunosensors. Different strategies are described ranging from three-dimensional matrices of polymers with multiple bioreceptor attachment sites to colloidal-enhanced surfaces (Hu et al., 2004; Lofas, 1995; Matsui et al., 2005). Periodic nano-structured surfaces are also recently introduced as novel SPR transduction substrates due to their unique optical properties.

Periodic structures (gratings) have been used in SPR biosensing since its early development. In some SPR systems, metallic gratings are employed to couple incident light into the surface plasmon waves. The gratings provide a mechanism to increase the illumination light momentum (Knoll, 1998). Today, interest in nano-structures also stems from the phenomenon of localized surface plasmon resonance of metallic particles on surfaces. These substrates are known to exhibit absorbance spectra that are sensitive to refractive index near the particles surface, and to the particle size and distribution (Haes and Van Duyne, 2004; Stuart et al., 2005). The latter can be used for biosensing applications once the particles are functionalized to capture a given biomolecule of interest.

Surface plasmon resonance biosensors utilise the excitation of a propagating electromagnetic (EM) wave (surface polariton or plasmon wave) to sense a binding event, the adsorption of the biomolecules of interest, at a metal-dielectric interface. Simply explained, at a metal-dielectric interface, the free electrons of the metal surface can support a collective oscillation, generating an associated EM wave (Raether, 1988). The oscillations are excited by an external illumination provided that the photon momen-

* Corresponding author at: Department of Biomedical Engineering, Montreal, Canada H3A 2B4. Tel.: +1 514 398 8129; fax: +1 514 398 7461.
*E-mail address:* maryam.tabrizian@mcgill.ca (M. Tabrizian).

0956-5663/$ – see front matter © 2009 Elsevier B.V. All rights reserved.
doi:10.1016/j.bios.2009.03.021

tum is matched to the wave vector of the surface plasmon wave. This is referred to as the resonance condition or resonance point. The latter is strongly dependent, among other system parameters, on the refractive index of the dielectric medium. Free-space photons require additional momentum in order to meet this resonance condition. The required momentum can be provided by a high index prism or as mentioned a grating structure. In the conventional prism coupler system (Kretschmann's configuration), the matching occurs at a given illumination wavelength and incident angle. As the refractive index of the dielectric medium changes, due to the adsorption of biomolecules, the resonance condition also changes, resulting in a measured resonance wavelength or angle shift. By tracking the resonance shift, one can correlate real-time measurements to the adsorption of the biomolecules. The plasmon waves are surface bound phenomena; as such, only local refractive index changes of the medium, close to the metal-dielectric interface are sensed. For a biosensor, the metal-dielectric interface is functionalized with surface bioreceptors, chosen for their specific affinity toward a given biomolecule to provide the biorecognition feature.

Functionalization techniques for SPR interfaces are numerous. These include long polymer chains of dextran (polysaccharide) featuring multiple bioreceptor attachment sites (Lofas, 1995), porous matrices with increased surface areas (Oh et al., 2006), and uniform self-assembled monolayers (Ulman, 1996). The patterning of the surface chemistry at the microscale and nanoscale is also extensively explored in the literature. Micro-contact printing, dip-pen nanotechnology, laser ablation and many others techniques are described (Coyer et al., 2007; Kirkwood et al., 2007; Lee et al., 2002; Rundqvist et al., 2007). Generally, they are employed to create substrates for cell-based biosensors and arrayed assays (DNA-chip, Bio-chip).

This article focuses on a novel functionalized biointerface featuring nano-structures, specifically zero-order gratings (nano-grating), placed on the medium or sample side of the metallic surface of a Kretschmann's SPR prism coupler configuration. Note that in this application, the nano-gratings are not used to couple light into the surface plasmon waves. Nano-gratings can perturb the propagation of the evanescent surface plasmon wave and generate a bandgap in its dispersion relation (Benahmed and Ho, 2007; Bonod et al., 2008; Fischer et al., 1994; Pincemin and Greffet, 1996). The bandgap represents a range of wavelengths or incident angles for which an incident light cannot excite a surface plasmon wave at the metal-dielectric interface (Barnes et al., 2003). It has been shown theoretically that for a biosensor operating near the bandgap, a multiple-fold increase in sensitivity is obtained when compared to a planar interface (Alleyne et al., 2007). Furthermore, the evanescent plasmon fields are redistributed on the surface such that areas of concentrated field intensity are created. This paper explores the possibility of further extending the sensitivity of this approach by guiding the immobilization of surface bioreceptors to specific sites on the nano-grating surface. The purpose is to create a patterned periodic immobilization to enhance the metallic nano-grating effect by concentrating the adsorption of bioreceptors on to areas of increased field intensity. In the following sections, the fabrication of the functionalized surface is first described. The technique uses a combination of electron-beam lithography, metal lift-off and self-assembled monolayers. Numerical studies are also carried out to predict the surface plasmon response and the field distribution. Finally, measurements on an imaging-SPR are carried out, using anti-TNF-α/TNF-α as a model bioreceptor/antigen, on the different fabricated substrates. TNF-α is a cytokine involved in the systemic inflammation response; it has been suggested that TNF-α can be used as a potential biomarker for the diagnosis of various diseases, including sepsis (Carrigan et al., 2004).

## 2. Materials and methods

### 2.1. Nano-structured SPR surface fabrication

In this paper, the design of a nano-structured and nano-patterned SPR interface employs Kretschmann's configuration given its simplicity and high sensitivity (Homola et al., 1999). The enhanced interface consists of a high index substrate coated with a thin layer gold, on which a binary 250 nm period gold nano-grating is introduced. The nano-gratings are 15 nm deep with 50% duty factor. The duty factor refers to the ratio of the grating mesa's width to its period. In this case, the mesas and troughs are of equal width. Once fabricated, the nano-structured and functionalized substrates can be placed atop the coupling prism of an existing SPR system for measurements. Surface bioreceptors constituting of antibodies are selectively immobilized exclusively on nano-grating mesas, on the trough or uniformly across the nano-grating and on a reference planar surface for comparative studies (Fig. 1).

The fabrication of the nano-structured and nano-patterned functionalized substrates is realised by electron beam lithography and a metal lift-off process. The details of the fabrication process have been presented in an earlier work (Hoa et al., 2008), which focuses on the characterization of nano-patterned surfaces using scanning near-field optical microscopy. The fabrication technique allows for the simultaneous fabrication of the gold nano-gratings and the selective immobilization of surface bioreceptors on the nano-grating mesa or trough with the passivation of substrate and the unfunctionalized nano-grating features. Four variations of the patterned interfaces are produced in this study, as shown in Fig. 1.

The SPR interfaces are fabricated on a high index planar substrate of SF11 glass (Schott). The fabrication starts with the deposition of a gold layer on the substrate with 3 nm of Cr for adhesion, followed by the deposition of a poly(methyl methacrylate) (PMMA) 150 nm bi-layer resist. The resist is then patterned by an electron-beam (LEO VP electronic microscope at 30 pA and 20 keV) over a 250 μm × 250 μm area with equally spaced 125 nm wide lines. For the reference planar interface (Fig. 1(d)), the entire 250 μm × 250 μm is exposed. The PMMA is then developed in isopropanol to reveal the written patterns. A 1 min quick oxygen plasma is applied to clean the surface. 3 nm of Cr is deposited; follow by a second deposition of gold, the thickness of which determines the nano-grating height.

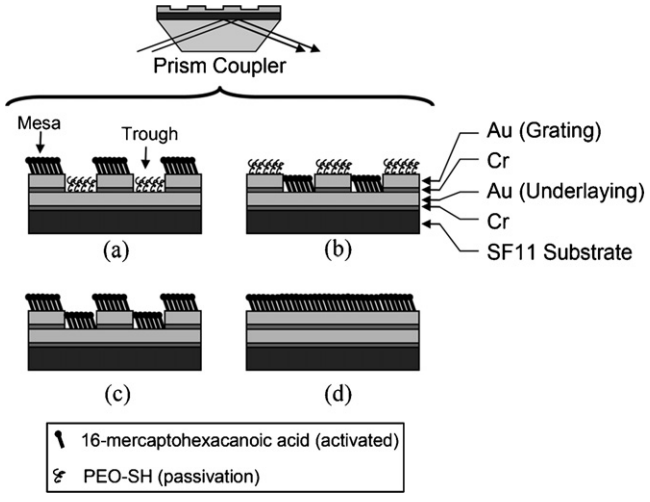


**Fig. 1.** Four biointerface designs (a) binary nano-grating with surface bioreceptors on the nano-grating mesas (b) with surface bioreceptors in the nano-grating troughs (c) uniformly distributed (d) reference surface with planar interface and functionalization.

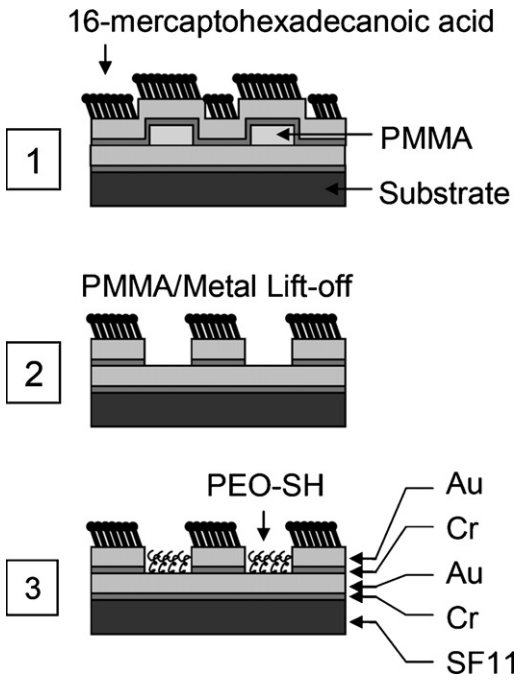


**Fig. 2.** Application of the surface chemistry for surface type (a). Step 1: Incubation of the first surface chemistry functionalizing the mesas. Step 2: metal lift-off in acetone/methyl ethyl ketone revealing the nano-grating troughs. Step 3: Application of the second surface chemistry to functionalize the troughs.

### 2.2. Differentiated surface chemistry on nano-gratings

The differentiated surface chemistry is realised using self-assembled monolayers of alkanethiol. A carboxilated alkanethiol, 16-mercaptohexadecanoic acid, is chosen for the attachment of protein bioreceptors. The carboxyl terminal is readily modified to an amine reactive succinimide-activated site, for which the attachment of proteins has been extensively demonstrated in the literature. For the passivation of the substrate and unfunctionalized nano-grating features against protein adsorption, a protein-repellent poly(ethylene) glycol thiolated self-assembled monolayer is applied.

The two-step functionalization is illustrated in Fig. 2 for the fabrication of the surface design of Fig. 1(a). The other surface designs are fabricated similarly by changing the order of the chemical used. The first surface chemistry, functionalizing the nano-grating mesa, is applied in an overnight incubation of either 1 nM of 16-mercaptohexadecanoic acid (Sigma–Aldrich) in ethanol (for Fig. 1(a)) or poly(ethylene) glycol thiols (Rapp Polymere) in water (for Fig. 1(b)). The patterned substrate is then rinsed with copious amounts of ethanol or water. A lift-off protocol (1 h incubation in 1:1 acetone/methyl ethyl ketone (MEK) solution at 40 °C, 1 min ultrasonication) is applied to remove the remaining PMMA, preserving the functionalized nano-grating mesa, but revealing the bare nano-grating trough. The substrate is then incubated in a second solution of 16-mercaptohexadecanoic acid (in ethanol) or poly(ethylene) glycol thiols (in toluene), depending on the existing mesa chemistry. This method functionalizes or passivates the exposed gold surface according to the desired design (Fig. 1). Finally, the carboxyl groups of the 16-mercaptohexadecanoic acid are activated with N-hydroxysuccinimide (NHS) (Fluka) in the presence of 1-(3-dimethylaminopropyl)-3-ethylcarbodiimide hydrochloride (EDC) (Fluka). The substrates are stored dry under nitrogen at 4 °C, prior to use. Surface characterization is performed by scanning electron microscopy (Hitachi SEM-S4700) and by phase-contrast atomic force microscopy (AFM, Veeco Nanoscope IIIa) for surfaces presenting differentiated functionalization on the nano-grating mesas and troughs (surface types of Fig. 1(a) and (b)). Phase-contrast AFM imaging can provide information on the composition and nature of surfaces (Jandt, 2001; Siedlecki and Marchant, 1998). In the phase-contrast mode, the phase lag between the oscillation of the AFM tip and the applied excitation signal is measured. It contains information pertaining to the interaction between the cantilever tip and the surface; and it allows the mapping and differentiation of surface composition, viscosity, hardness, elasticity or adhesion (Chen et al., 1998; Siedlecki and Marchant, 1998). For the purpose of characterizing the differentiated surface chemistry on the nano-gratings, quantum-dots – antibody conjugate (Qdot® 655 rabbit F(ab')2 anti-goat IgG conjugates, Invitrogen) is adsorbed onto the EDC/NHS activated 16-mercaptohexadecanoic acid. The quantum-dots are used to provide an additional difference in surface-tip interaction to the 16-mercaptohexadecanoic acid/poly(ethylene) glycol thiol surface, with respect to surface hardness and composition.

### 2.3. Modelling of nano-structured SPR biointerface

As stated, periodically structured metallic surfaces are known to perturb the propagation of the surface plasmon wave, and introduce a bandgap in the dispersion relation. The bandgap is a region where coupling to the surface plasmon does not occur at any wavelength or angle of incident (absence of resonance condition). In simulation, improved SPR sensitivity has been observed close to the bandgap (Alleyne et al., 2007). Due to the presence of nano-gratings, the evanescent field of the surface plasmon is also redistributed with field concentration strongest at the grating edges and mesas.

A proprietary implementation of the rigorous coupled-wave analysis (DiffractMOD) method is employed in the numerical study of the surface plasmon resonance response of the nano-patterned and nano-structured surfaces. The technique has been previously reported for this type of computations (Moharam et al., 1995; Moharam and Gaylord, 1985; Moharam and Gaylord, 1986).

The 250 nm period nano-grating with 50% duty factor interface is composed of a high refractive index glass substrate (prism) and a multilayer stack that is comprised of the 3 nm Cr layer for adhesion, 25 nm of underlaying gold, another 3 nm of Cr and 15 nm of gold for the nano-grating structure, as fabricated. An illumination wavelength of 810 nm is used to match that of the experimental setup. The optical properties of the glass and metals are taken from the manufacturer and Johnson and Christy (Johnson and Christy, 1972, 1974), respectively. The four functionalization patterns as illustrated in Fig. 1 are simulated. In our model, the adsorption of biomolecules is represented as a refractive index change in the first 10 nm above the nano-grating surface from a background index of 1.33–1.60

### 2.4. Imaging-SPR measurements

The SPR angular responses of the four fabricated substrates are obtained for the adsorption of a model bioreceptor-analyte (anti-TNF-α/TNF-α). For the experimental verification, an imaging-SPR (SPRi-lab, Genoptic) is used. The imaging-SPR approach expands the measuring capability of standard SPR biosensors by allowing the measurement of the plasmon resonance response over a two-dimensional area of the substrate. Imaging-SPR systems are designed for applications in genomics or proteomics where large arrays of surface receptors are measured simultaneously. In this experiment, the average SPR response over the 250 μm × 250 μm nano-structured surfaces is measured. In most imaging systems (Phillips and Cheng, 2007) (Fig. 3), the laser of the typical SPR is replaced with a collimated illumination source from a light emitting diode (LED). A detector array (CCD camera) is used to collect the reflected light from the gold substrate. Generally, a

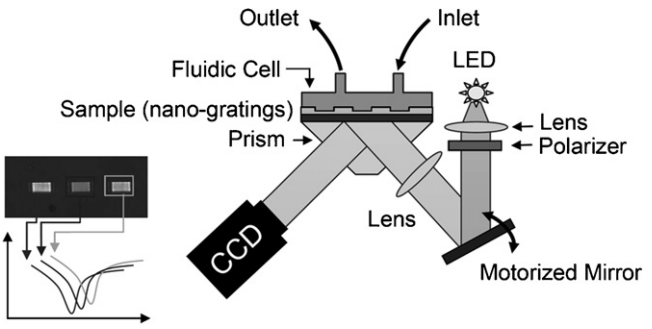


**Fig. 3.** Imaging-SPR measurement setup.

fixed wavelength and incident angle are chosen. The adsorption of biomolecules is measured as a change in the intensity of the reflected light. Alternatively, surface plasmon reflectance curves can be measured for each pixel element or averaged over a subset of pixels by scanning over an incident angle range using a motorized rotating mirror.

The fabricated substrates are placed on the SPRi-lab's coupling prism with matching index immersion oil (Cargille Labs) to minimize reflective losses at the prism-substrate interface. A peristaltic pump circulates phosphate buffer saline (PBS, pH 7.4) through the fluidic system at 100 μL/min and fills the fluidic cell. Using the polarizer, a scan in transverse-electric (TE)-polarisation is first performed of the surface for data normalization. The surface plasmon resonance curves are then measured in transverse-magnetic (TM)-polarisation light, as surface plasmon waves are only excited in this polarisation. Successive 1 mL solutions of anti-TNF-α (Peprotech) in PBS/acetate (Sigma–Aldrich) with increasing concentration (1 μg/mL, 2 μg/mL) are injected into the fluidic system. The increasing solution concentration of anti-TNF-α leads to higher surface concentrations, thus increased surface refractive index. Acetate buffer is added to the PBS to lower its pH to aid the adsorption by working below the antibody's isoelectric point. As the anti-TNF-α adsorption reaches equilibrium, PBS buffer is reintroduced into the fluidic cell and the plasmon resonance curves are measured. For the adsorption measurements (kinetic curves), the reflectivity intensity is tracked at a fixed angle (58°). After each injection, the angular SPR shifts are calculated for the four surfaces. The surface plasmon curves are fitted to a second order polynomial and the minima (polynomial zeros) are extracted. The experiments are repeated in triplicate and averaged, with the error taken as the standard deviation. Samples are used once and are not regenerated.

## 3. Results and discussion

### 3.1. Surface characterization

The SEM micrograph of the fabricated nano-grating is shown in Fig. 4(A). Good periodic structures with 125 nm line width for both the trough and mesa are obtained. The line edges are not as smooth as one would desire due to the lift-off process, and are expected to add noise to the surface plasmon resonance measurements. However, consistent lift-off is obtained for the entire fabricated surface of 250 μm × 250 μm. The PMMA bi-layer approach for the E-beam patterning, as described in (Hoa et al., 2008) facilitates the metal lift-off by providing an undercut structure and thus allowing solvent access to the PMMA resist when incubated in the acetone/MEK bath.

The phase-contrast images of the quantum-dots on the nano-grating mesa Fig. 4(C)) and quantum-dots on the nano-grating trough (Fig. 4 (E)) clearly demonstrate the differentiated surface chemistry. Compared to the topographic images (Fig. 4(B)), Fig. 4(D)), respectively, the adsorptions are well correlated to the nano-grating features, with some level of non-specific adsorption of the antibody on the poly(ethylene) glycol functionalized areas. An additional characterization by measuring the local emission of the patterned quantum-dots is also completed; results of this measurement have already been presented in (Hoa et al., 2008). The planar surface and uniformly functionalized nano-gratings (Fig. 1(c) and (d)) do not present differentiated surface chemistry and thus are not measured here.

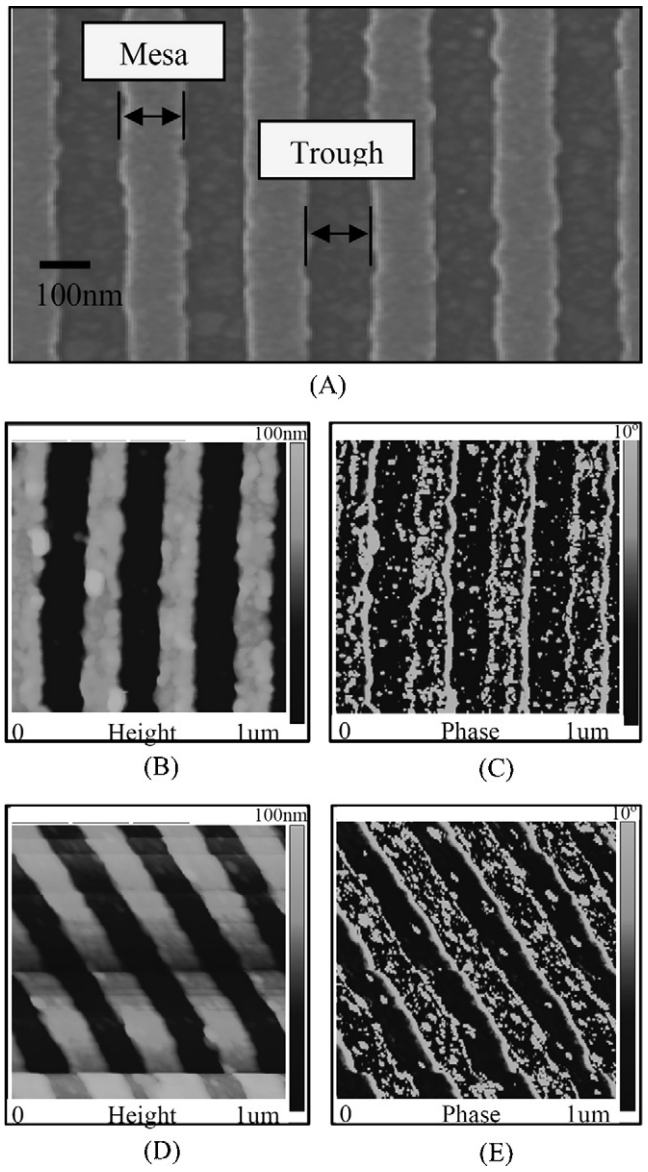


**Fig. 4.** (A) SEM micrograph of gold nano-grating showing good 125 nm features and 50% duty factor. Phase-contrast AFM measurements, (B) topographic image of biointerface nano-grating with active chemistry (bioreceptor/antibody-qdots) on mesa, (C) phase-contrast image, (D) topographic image of biointerfaces with active surface chemistry in the trough (note that the dark horizontal bans are measurement artefacts), (E) phase-contrast image.

### 3.2. Numerical results of SPR angular response

Generally, the planar interface results in a narrow resonance reflectivity dip, while corrugated interfaces broaden it. Fig. S1 (supplemental content) depicts the SPR angular response of both the planar interface and the 250 nm nano-grating interface from the rigorous coupled-wave analysis. Furthermore, the surface plasmon

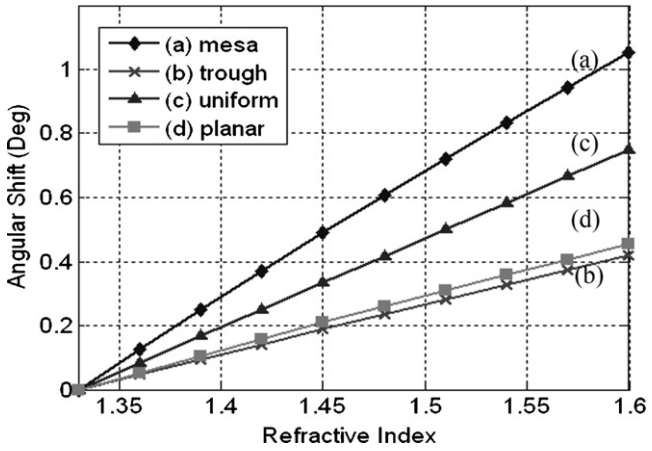


**Fig. 5.** RCWA angular resonance shift for the four interface configurations. Letters refer to surface types illustrated in Fig. 1.

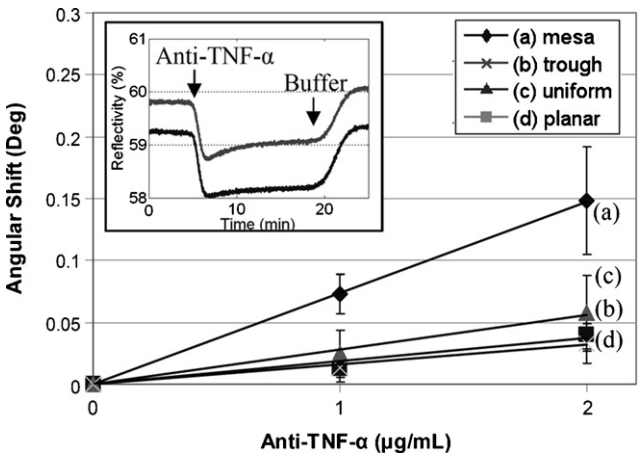


**Fig. 6.** Angular shift (deg) after the injection of 1 μg/mL anti-TNF-α and injection of 2 μg/mL concentration. (Insert) Adsorption kinetic of 2 μg/mL of anti-TNF-α. The letters refer to the patterned functionalization, as illustrated in Fig. 1.

electromagnetic field distribution (Fig. S1 (insert), supplemental content) for the corrugated surface shows a concentration of field intensity ($E_z$) localized on the nano-grating mesa, with peak concentration at the edge of the gratings. For biosensors operating at fixed wavelength and incident angle, where the reflectivity intensity changes are measured and correlated to the surface adsorption, the narrower response is preferred. However for biosensors operating in the angular interrogation mode, the simulations show that the angular shift response of the corrugated surface compared to a planar interface is increased by multiple folds (Fig. 5).

The numerical results point to an almost three times improvement in the angular response when compared to the planar interface. And in comparison to a uniformly functionalized nano-grating, a 40% larger SPR response is also observed, attributed to the concentration of adsorbed biomolecules in the regions of high field intensity. For fair comparison, the effective refractive index changes on the surface over the entire 250 μm × 250 μm area are equal for all four surfaces, so as to model a similar overall surface adsorption density. Note that the simulated refractive index change represents a large range. In reality, the adsorption induces a significantly smaller refractive index change ($<1 \times 10^{-2}$). However, as shown in Fig. 5, the angular response or shift is linear over the entire range of refractive indexes, thus suggesting that it is suitable for various applications, where non-aqueous solutions with a higher index may be used.

### 3.3. *Anti-TNF-α adsorption*

Fig. 6 (insert) shows the adsorption kinetic for the injection of 2 μg/mL of anti-TNF-α. A large reflectivity change is first measured at the moment of injection due to the bulk buffer change from PBS buffer to PBS/Acetate buffer. The adsorption then follows an exponential increase and reaches equilibrium. A final large upward shift in reflectivity intensity is observed with the injection of the PBS buffer.

The measured surface plasmon resonance shifts, Fig. 6 and Fig. S2 (supplemental content), for the four different surfaces show that the nano-gratings with the surface bioreceptors (antibody) adsorbed on the mesas provides the largest resonance shift (a), as suggested by the numerical model. Fig. S2 presents the incremental change for each successive injection of 1 μg/mL and 2 μg/mL of anti-TNF-α to the surfaces; and shows a similar incremental change for each injection, suggesting a doubling of surface density. Fig. 6 shows the total surface plasmon resonance shift after each injection. The trends for the nano-grating surface with antibodies adsorbed uniformly across the nano-gratings (Fig. 1(c)), uniquely in the troughs (Fig. 1(b)), and on the planar surface (Fig. 1(d)), show decreasing resonance shifts. While the results for surface (b), (c) and (d) are inconclusive given the size of the error bars, the responses to increased solution concentrations show a higher slope, thus increased sensitivity, for the functionalized nano-grating mesas. The response for the uniformly functionalized surface suggests that, in this case, the bioreceptors bind significantly in the nano-grating trough as the SPR response is closer to that of case (b) for which the nano-grating mesas are passivated against adsorption. The latter experimental results point to the advantage of patterning the surface functionalization and concentrating the biomolecules to areas of increased field concentration. Note that to ensure similar adsorption surface densities for each surface, the same functionalization conditions are applied to the samples (exposure to similar solvents, incubation times, and ultrasonication). Furthermore, the nano-grating troughs are relatively shallow (15 nm) and wide (125 nm) compared to an antibody and thus should minimise any hindrance effect of the surface topography. In this study, differences between experimental and simulated results are also expected due to imperfections in the fabrication process and also arise from the non-perfect differentiated functionalization. Non-specific adsorption adds noises to the measurements and also dampens the adsorbed biomolecule concentration effects. Differences also arise from discrepancies between material properties (refractive indexes) used in the simulations and those of the actual materials.

In addition to the electromagnetic enhancement and the concentration of biomolecules, the nano-gratings and patterned functionalized may increased the accessibility of the analytes, TNF-α, to the anti-TNF-α bioreceptors. In particular, for surface bioreceptors adsorbed on the mesa edges, the bioreceptors are not constricted to a two-dimensional plane, thus increasing the probability of binding with their target. It is believe to have a similar effect to that reported by others using nano-particles or dentritic surface as substrates for antibody immobilization (Liao, 2007; Wang et al., 2004). Furthermore, as shown in Fig. S1(insert), the electromagnetic fields are strongly concentrated at the mesas' edge. This can provide a synergic effect to the sensitivity improvement. This is observed for the injection of 1 μg/mL of TNF-α (Peprotech) in PBS (Fig. S3, supplemental content) to the surfaces with pre-adsorbed anti-TNF-α bioreceptors on the nano-grating surface (mesas) and the planar surface. One observes a mean increase by a factor of approximately of 8 in the angular shift for the binding of the antigen (TNF-α), while only a factor of 4–5 is measured for the adsorption of anti-TNF-alpha when comparing the functionalized grating mesas

to the planar surface (Fig. 6). In the latter case, the biomolecules (anti-TNF-α) were expected to adsorb directly and uniformly onto the self-assembled monolayer, as opposed to the TNF-α that are hypothesized to be more readily captured by the bioreceptors at the grating edges. In the latter measurements as in the results for the anti-TNF-α, the sample-to-sample variability is larger than one would desire. The large variability is suspected to be due mainly to the edge effects. As shown, the grating edges are not smooth and thus can add noises to the measurements from sample to sample. The fabrication also introduces small variations in the grating duty cycle and period which affect the surface plasmon resonance response. Improvements in the fabrication processing, particularly to choice (molecular weight, bi-layer structure) and design of the pattern PMMA resist can minimize these effects. Furthermore, surface chemistry optimization with respect to the choice of molecules, solvent, incubation times can also minimize non-specific adsorption the surfaces. In particular, improving the lift-off process in the fabrication process to avoid or minimise harsh incubations or ultrasonication can ease the constraints on the application of the surface chemistry and allow for improved mesa/trough functionalization and passivation.

## 4. Conclusions

The selective immobilization of surface bioreceptors to match the mapping of the electromagnetic field distribution of a surface plasmon resonance biointerface is demonstrated, numerically and experimentally to be advantageous leading to a sensitivity enhancement in the design of biosensors. The concentration of the limited biomolecules to areas of high field strength is demonstrated to produce a larger angular resonance shift. It is known that the geometry and distribution of the nano-gratings and other nano-structures determine the surface plasmon field distribution (Bonod et al., 2008; Byun et al., 2006). For example, designs can be implemented to concentrate field strength at the apex of a three-dimensional layer (Chien and Szkopek, 2008). In this instance, the work presented here points to the advantage in concentrating the surface bioreceptors. As presented in this paper, the fabrication required the patterning of a thin polymer resist film by electron-beam lithography. The process can be time-consuming and costly; however, the literature describes several alternative fabrication techniques for the patterning of a polymer resists with nanometric feature sizes (Gates et al., 2005). For low-cost mass production, the use of a master template in a stamping technique to pattern a polymer resist instead of the electron-beam as been demonstrated elsewhere (Faircloth et al., 2000), and could be applied to the approach presented here. This latter development combined with the careful design of the functionalized biointerfaces using nanotechnology is critical for the development of sensitive integrated SPR biosensors and platforms for in-field applications.

## Acknowledgements

The authors would like to acknowledge the following agencies for funding: Le Fonds Québécois de la Recherche sur la Nature et les Technologies (FQRNT), Team grant and regroupement stratégique grant, NanoQuébec and the Natural Sciences and Engineering Research Council of Canada (NSERC)-CRD program. The authors also acknowledge the contribution of Alvaro Jimenez, Dr. Matthieu Martin, Dr. Paul Charette and Dr. Jacques Beauvais (University de Sherbrooke, Département de génie électrique et de génie informatique) for their collaboration in the fabrication and characterization of the nano-grating surface.

## Appendix A. Supplementary data

Supplementary data associated with this article can be found, in the online version, at doi:10.1016/j.bios.2009.03.021.

## References

Alleyne, C.J., Kirk, A.G., Nicorovici, N.-A.P., Maystre, D., 2007. Opt. Express 15 (13), 8163–8169.
Barnes, W.L., Dereux, A., Ebbesen, T.W., 2003. Nature 424 (6950), 824–830.
Benahmed, A.J., Ho, C.M., 2007. Appl. Opt. 46 (16), 3369–3375.
Bonod, N., Popov, E., McPhedran, R.C., 2008. Opt. Express 16 (16), 11691–11702.
Byun, K.M., Kim, D., Kim, S.J., 2006. Sens. Actuators B: Chem. 117 (2), 401–407.
Carrigan, S.D., Scott, G., Tabrizian, M., 2004. Clin. Chem. 50 (8), 1301–1314.
Chen, X., Davies, M.C., Roberts, C.J., Tendler, S.J.B., Williams, P.M., Davies, J., Dawkes, A.C., Edwards, J.C., 1998. Ultramicroscopy 75 (3), 171–181.
Chien, W.Y., Szkopek, T., 2008. Opt. Express 16 (3), 1820–1835.
Coyer, S.R., Garcia, A.J., Delamarche, E., 2007. Angew. Chem.-Int. Ed. 46 (36), 6837–6840.
Faircloth, B., Rohrs, H., Tiberio, R., Ruoff, R., Krchnavek, R.R., 2000. J. Vac. Sci. Technol. B 18 (4), 1866–1873.
Fischer, B., Fischer, T.M., Knoll, W., 1994. J. Appl. Phys. 75 (3), 1577–1581.
Gates, B.D., Xu, Q.B., Stewart, M., Ryan, D., Willson, C.G., Whitesides, G.M., 2005. Chem. Rev. 105 (4), 1171–1196.
Haes, A.J., Van Duyne, R.P., 2004. Anal. Bioanal. Chem. 379 (7–8), 920–930.
Hoa, X.D., Martin, M., Jimenez, A., Beauvais, J., Charette, P., Kirk, A., Tabrizian, M., 2008. Biosen. Bioelectron. 24 (4), 976–981.
Homola, J., Koudela, I., Yee, S.S., 1999. Sens. Actuators B: Chem. 54 (1–2), 16–24.
Hu, W.P., Chen, S.J., Huang, K.T., Hsu, J.H., Chen, W.Y., Chang, G.L., Lai, K.A., 2004. Biosens. Bioelectron. 19 (11), 1465–1471.
Jandt, K.D., 2001. Surface Sci. 491 (3), 303–332.
Johnson, P.B., Christy, R.W., 1972. Phys. Rev. B. 6 (12), 4370–4379.
Johnson, P.B., Christy, R.W., 1974. Phys. Rev. B. 9 (12), 5056.
Kirkwood, S.E., Shadnam, M.R., Amirfazli, A., Fedosejevs, R., 2007. J. Phys.: Conference Series 59, 428–431.
Knoll, W., 1998. Ann. Rev. Phys. Chem. 49, 569–638.
Lee, K.B., Park, S.J., Mirkin, C.A., Smith, J.C., Mrksich, M., 2002. Science 295 (5560), 1702–1705.
Liao, J.Y., 2007. Colloids Surf. B: Biointerfaces 57 (1), 75–80.
Lofas, S., 1995. Pure Appl. Chem. 67 (5), 829–834.
Matsui, J., Akamatsu, K., Hara, N., Miyoshi, D., Nawafune, H., Tamaki, K., Sugimoto, N., 2005. Anal. Chem. 77 (13), 4282–4285.
Moharam, M.G., Gaylord, T.K., 1985. J. Opt. Soc. Am. A: Opt. Image Sci. Vision 2 (13), 99.
Moharam, M.G., Gaylord, T.K., 1986. J. Opt. Soc. Am. A: Opt. Image Sci. Vision 3 (11), 1780–1787.
Moharam, M.G., Grann, E.B., Pommet, D.A., Gaylord, T.K., 1995. J. Opt. Soc. Am. A: Opt. Image Sci. Vision 12 (5), 1068–1076.
Oh, S., Moon, J., Kang, T., Hong, S., Yi, J., 2006. Sens. Actuators: B Chem. 114 (2), 1096–1099.
Phillips, K., Cheng, Q., 2007. Anal. Bioanal. Chem. 387 (5), 1831–1840.
Pincemin, F., Greffet, J.J., 1996. J. Opt. Soc. Am. B: Opt. Phys. 13 (7), 1499–1509.
Raether, H., 1988. Surface Plasmons on Smooth and Rough Surfaces and on Gratings. Springer-Verlag, Berlin.
Rundqvist, J., Mendoza, B., Werbin, J.L., Heinz, W.F., Lemmon, C., Romer, L.H., Haviland, D.B., Hoh, J.H., 2007. J. Am. Chem. Soc. 129 (1), 59–67.
Siedlecki, C.A., Marchant, R.E., 1998. Biomaterials 19 (4–5), 441–454.
Stuart, D.A., Haes, A.J., Yonzon, C.R., Hicks, E.M., Van Duyne, R.P., 2005. Nanobiotechnology, IEEE Proceedings, vol. 152 (1), pp. 13–32.
Ulman, A., 1996. Chem. Rev. 96, 1533–1554.
Wang, H., Liu, Y., Yang, Y., Deng, T., Shen, G., Yu, R., 2004. Anal. Biochem. 324 (2), 219–226.